

## APPLICATION OF ECR ION SOURCE BEAMS IN ATOMIC PHYSICS

F. W. MEYER

Oak Ridge National Laboratory,\* Oak Ridge, Tennessee 37831

The availability of intense, high charge state ion beams from ECR ion sources has had significant impact not only on the upgrading of cyclotron and synchrotron facilities, but also on multicharged ion collision research, as evidenced by the increasing number of ECR source facilities used at least on a part time basis for atomic physics research. In this paper one such facility, located at the ORNL ECR source, and dedicated full time to the study of multicharged ion collisions, is described. Examples of applications of ECR ion source beams are given, based on multicharged ion collision physics studies performed at Oak Ridge over the last few years.

Introduction

While developed initially as an injector for high energy accelerators, the ECR ion source has in recent years become an indispensable tool in the field of multicharged ion collision physics. In fact, the availability of low energy, intense, high charge state ion beams of high duty factor from ECR sources has opened many areas of multicharged ion research that have previously been inaccessible. Examples include investigations of low energy collisions involving bare ions of  $Z > 5$ , merged beams experiments, studies of electron-ion collisions, and investigations of multicharged ion-surface interactions. Due to their great utility in atomic physics research, a number of ECR sources, listed in Table I, are now available, at least part time, for use in the study of multicharged ion collisions.

At Oak Ridge an ECR source has been in operation since 1984, completely dedicated for use in atomic physics studies. In the first part of this paper the present configuration of the ORNL ECR source, as well as current source performance will be described. Recent experience in metal ion production will also be summarized. In the subsequent sections, some atomic physics experiments carried out at the ORNL ECR source facility will be described, illustrating the utility of ECR sources in the study of ion-atom, and electron-ion collisions, as well as of ion-surface interactions.

\*The submitted manuscript has been authored by a contractor of the U.S. Government under contract DE-AC05-80OR21400. Accordingly, the U.S. Government retains a certain number of reproduction rights to publish or reproduce the published form of this contribution, or allow others to do so, for U.S. Government purposes."

MASTER

Table I. ECR-source-based atomic physics programs

Place	Year Est.	Source(s)	Avail.	Program
Grenoble (PADSI/AGRIPPA)	1980	10 GHz MINIMAFIOS	Full	Ion-atom, spectroscopy, surfaces
	1985	16 GHz MINIMAFIOS	Part	
	1986	10 GHz FERROMAFIOS	Part	
KVI Groningen	1982	10 GHz MINIMAFIOS	Part	Ion-atom, surfaces, spectroscopy
Louvain-la-Neuve	1983	8.5 GHz OCTOPUS	Part	Ion-electron Ion-atom
Oak Ridge	1984	10.6 GHz ORNL ECR	Full	Ion-atom, ion-electron, ion-ion, surfaces, spectroscopy
Berkeley	1985	6.4 GHz LBL ECR	Part	Ion-atom, spectroscopy
Giessen	1986	5 GHz PRE-ISIS	Full	Ion-atom, ion-electron, ion-ion, spectroscopy
Argonne	1987	10.5 GHz PIIECR	Part	Ion-atom, spectroscopy

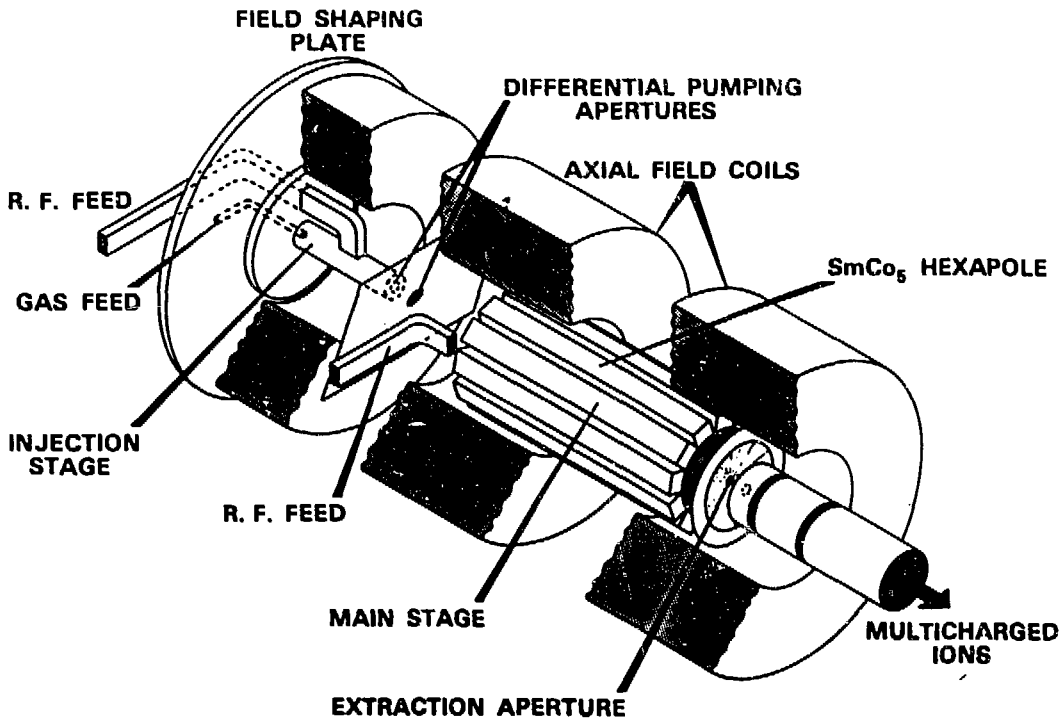
### DISCLAIMER

This report was prepared as an account of work sponsored by an agency of the United States Government. Neither the United States Government nor any agency thereof, nor any of their employees, makes any warranty, express or implied, or assumes any legal liability or responsibility for the accuracy, completeness, or usefulness of any information, apparatus, product, or process disclosed, or represents that its use would not infringe privately owned rights. Reference herein to any specific commercial product, process, or service by trade name, trademark, manufacturer, or otherwise does not necessarily constitute or imply its endorsement, recommendation, or favoring by the United States Government or any agency thereof. The views and opinions of authors expressed herein do not necessarily state or reflect those of the United States Government or any agency thereof.

## The ORNL ECR Source

In order to permit extension of studies of the atomic physics of multicharged ion collisions started in our laboratory in 1975, an ECR ion source was built at ORNL which became operational early in 1984. The initial operation of the ORNL ECR source has been previously described.<sup>1</sup> While far from optimized in its first year of operation, the ion source was nevertheless already able to provide fully stripped ion beams of C, N, O, F, and Ne of sufficient stability and intensity to permit electron capture cross section measurements using an atomic hydrogen target.<sup>2</sup> Optimization of the source, particularly of the first stage, occurred intermittently over the period of a year starting in late 1984 and resulted in improved ion beam intensity and stability, facilitating the first crossed beams<sup>3</sup> and merged beams<sup>4</sup> experiments carried out using the source. In 1985 iron ion beams were developed and used for a comprehensive crossed beams study<sup>5</sup> of electron impact ionization along the Fe isonuclear sequence from charge 5+ to 15+. In 1987, ion beams of the refractory metals, including Ti, W, and Ta, as well as of other high melting point metals, such as Cr, Ni, and Au, were obtained. In the meantime, the repertoire of experiments carried out with the ORNL ECR source has steadily expanded and includes now a merged beams experiment studying charge transfer at very low energies, high resolution spectroscopic measurements of Auger electrons emitted during multicharged ion-atom collisions, and investigations of multicharged ion-surface interactions at low energies.

The salient features of the ORNL ECR source are shown in Fig. 1 (present source parameters are summarized elsewhere<sup>6</sup>). The source operates at a microwave frequency of 10.6 GHz and consists of two stages. The first stage, essentially a preionizer, consists of a 2.5 cm diameter circular waveguide, and generates singly charged ions (and electrons) in an ECR discharge, which then drift into the second or main stage of the ion source. The second stage is separated from the (high pressure) first stage by two stages of differential pumping, which is sufficient to maintain low  $10^{-6}$  Torr operating pressure. The second stage serves to confine energetic electrons that are heated by resonant microwave absorption. By collisions with these "hot" electrons, the singly charged ions are stripped to the high charge states that are then extracted from the source. The first stage ECR plasma electrons are weakly confined in an axial magnetic mirror.



ORNL ECR Multicharged Ion Source

Fig. 1. Cutaway drawing of the ORNL ECR source.

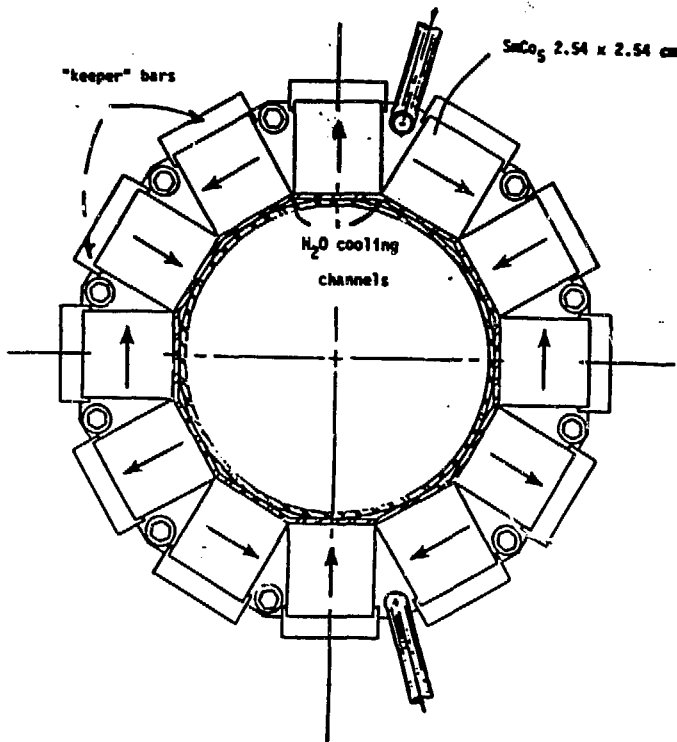


Fig. 2. Cross sectional view of SmCo<sub>5</sub> permanent magnet hexapole assembly; arrows indicate magnetization axis.

An iron plate in back of the first stage provides a region of high magnetic field where the first stage microwave vacuum window is located. The second stage ECR plasma electrons are confined in a "minimum B" configuration produced by superposition of an axial magnetic mirror field and a radial magnetic hexapole field. The hexapolar field is produced by a compact assembly of SmCo<sub>5</sub> permanent magnets positioned around the cylindrical vacuum wall of the second stage. The hexapolar magnetic field strength at the vacuum wall is about 4 kG. Figure 2 shows a cross sectional view of the 12-piece hexapole magnet assembly. Cooling of the permanent magnets is achieved by water circulation through the voids created between the cylindrical vacuum wall and the duodecagon defined by the SmCo<sub>5</sub> bars.

The multicharged ions escaping through the 0.8 cm aperture in the plasma electrode at the end of the main stage are formed into an ion beam using a "Pierce-like" extraction geometry. The ions are accelerated across a 2.6 cm gap to a "puller" electrode with 1.0 cm aperture. For optimum beam currents, the puller electrode requires negative biasing of at least a few hundred V. An Einzel lens located 50 cm downstream and operated in "accel" mode<sup>7</sup> focuses the extracted beam onto the entrance aperture of a stigmatic 90° magnetic charge analyzer having a 40 cm radius of curvature.

The ECR source was designed for a maximum source potential of 20 kV. Beam divergences have been measured using a rotating wire beam scanner located about 1 m after the exit slits of the 90° charge analyzer. For 50 keV O<sup>5+</sup> beams, the divergence half angles of the central 2x2 mm portion of the ion beam were measured to be 12 and 8 mr, in the horizontal and vertical planes, respectively. The full analyzed beam intensity is usually obtained when the analyzer slits are opened to 10x10 mm. Low energy ion beams have been extracted at source potentials as low as 400 V. At energies below about 5xq keV, the magnetic fringe field of the ECR source contributes significantly to the focusing of beams having low magnetic rigidity. Until early 1987, beams from the ECR source could be delivered to only one "user port," located about 1.5 m after the exit slit of the charge analyzer. A half scale version of the main 90° charge analyzer has been installed in the meantime, which can be used to switch the beam between the original straight-through beamline and one oriented at 90° to it. A rotatable spherical-sector electrostatic 90° deflector installed at the end of the new beamline provides two additional user ports. The resulting total of

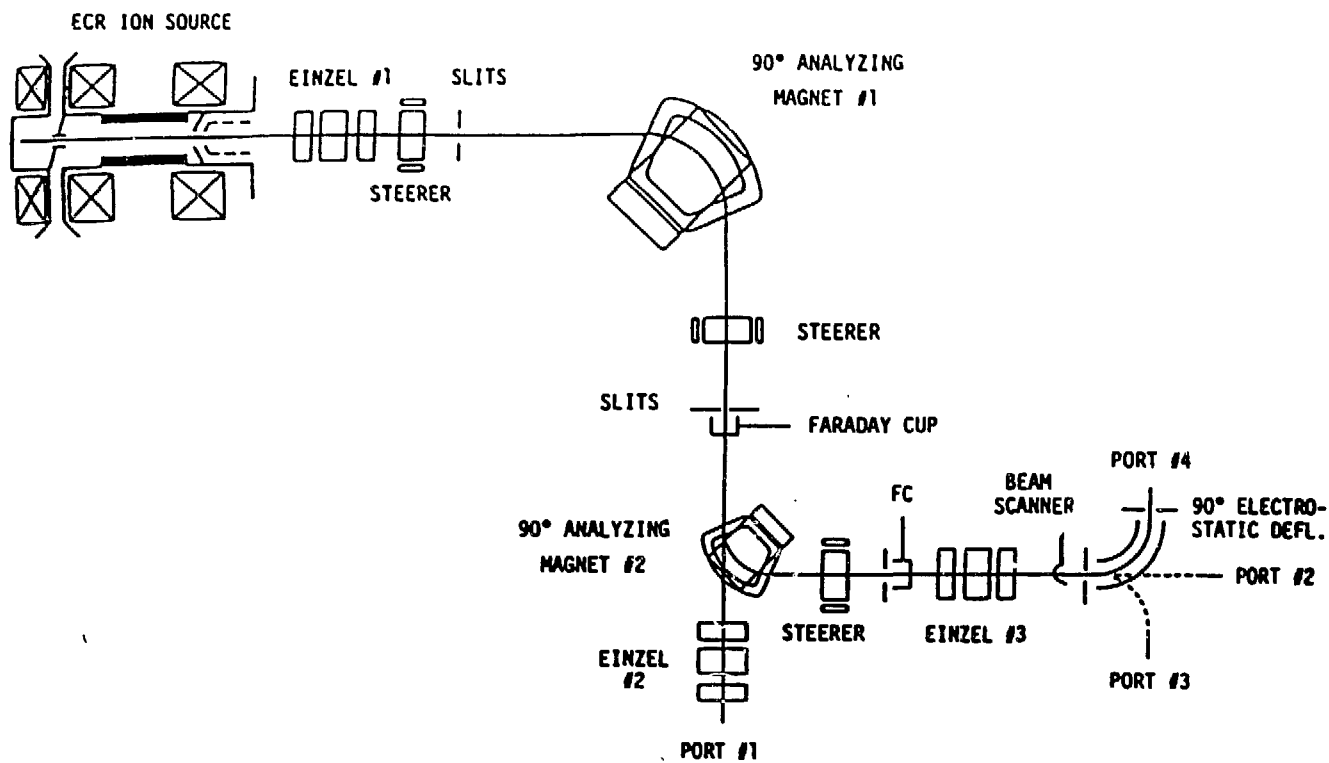


Fig. 3. Beamline layout of ORNL ECR source facility.

four beamlines, all designed for maximum beam transmission, are shown schematically in Fig. 3, and have greatly increased the flexibility and accessibility of the ECR source facility.

Table II summarizes typical beam currents obtained using the ORNL ECR source for a few representative elements. Ions of elements existing as permanent gases are straightforward to produce. Gas mixing was used to obtain maximum beam currents in the high charge state tail of the charge state distribution. He or H<sub>2</sub> was found to be effective for the lighter elements (A<20). N<sub>2</sub> or O<sub>2</sub> were used with the heavier elements. Ions of the metallic elements were produced using a solid feed technique similar to that described by Delaunay et al.<sup>6</sup> The technique entails inserting a small metallic sample into the ECR plasma, thereby heating the sample by electron impact and raising the vapor pressure of the sample sufficiently to yield useable ion beam currents. Most of the metallic samples used were in the form of thin foils (0.025-0.25 mm thick), to minimize the thermal time constant that determines the rate of sample heating, and also to minimize thermal conduction away from the foil edge in contact with the plasma, while maximizing the surface area from which vaporization occurs. The rate of vaporization is determined by the local electron power density seen by the sample, and can thus be varied by changing the foil position, tuning the source magnetic field, or adjusting the microwave power.

In the case of the Fe and Ni beams, non-magnetic samples of stainless steel and Inconel were used to avoid mechanical stresses due to the magnetic fields confining the main stage ECR plasma. Inconel could also be used to produce copious beams of Cr. "Mix" gases of nitrogen or oxygen were used to sustain the main stage plasma in the absence of metal vapor, and to optimize the high charge states as mentioned above. When using the Inconel foil sample for Ni beams, the use of O<sub>2</sub> was found to result in significant oxide formation on the foil, which inhibited sample vaporization and resulted in erratic and unstable ion beams. The situation was significantly improved after switching to N<sub>2</sub>. A similar effect was not observed when using O<sub>2</sub> with stainless steel foils. A typical consumption rate measured for the stainless steel foil samples was 3.5 mg/hr.

Ta ions could be produced either from a 0.025 mm thick foil or from the Ta liner protecting the vacuum wall of the second stage. The latter method required lowering the solenoidal magnetic field in the second stage,

Table II. Representative ORNL ECR source beam currents  
(electrical  $\mu\text{A}$ ); 10-12 kV source voltage.

	160	$^{40}\text{Ar}$	$^{56}\text{Fe}$	$^{58}\text{Ni}$	$^{84}\text{Kr}$	$^{127}\text{I}$	$^{129}\text{Xe}^{\text{a}}$	$^{181}\text{Ta}$	$^{197}\text{Au}$
+1	400	110	10						
+2	300	120	*						
+3	170	90	20						
+4	100	75	*						
+5	83	*	23	3	20				
+6	50	65	25	5	25				
+7	2.5	73	*	7	26				
+8	0.1	105	*	12	27				
+9		45	20	20	33		5.0		
+10		*	10	17	31	8	4.5	12	25
+11		3.0	5	*	33	10	3.5	*	27
+12		0.7	*	5	40	14	3.5	12	21
+13			2	3	23	18	3.2	12	18
+14			*	1	21	20	2.5	12	*
+15			1.5	0.5	15	18	1.5	12	18
+16				0.15	5	*	1.2	12	15
+17				0.03	1	10	1.0	11	12
+18					*	*	0.6	8	10
+19					0.25	3	0.6	5	7
+20						2	0.5	3.5	5
+21						*	0.25	2	5
+22						0.5	0.12	1.8	4
+23								*	3
+24								1.5	2.5
+25							0.08	1.0	*
+26							0.05	*	0.9
+27								0.4	0.4
+28								0.1	*
+29								0.05	0.1
+30									0.015 <sup>b</sup>
+31									0.005 <sup>b</sup>

\* Indicates m/q degeneracy with contaminant beam.

<sup>a</sup> 5 x 5 mm slits.

<sup>b</sup> 2 x 2 mm slits.



## CHARGE STATE DISTRIBUTION OF Au IONS FROM ORNL ECR SOURCE

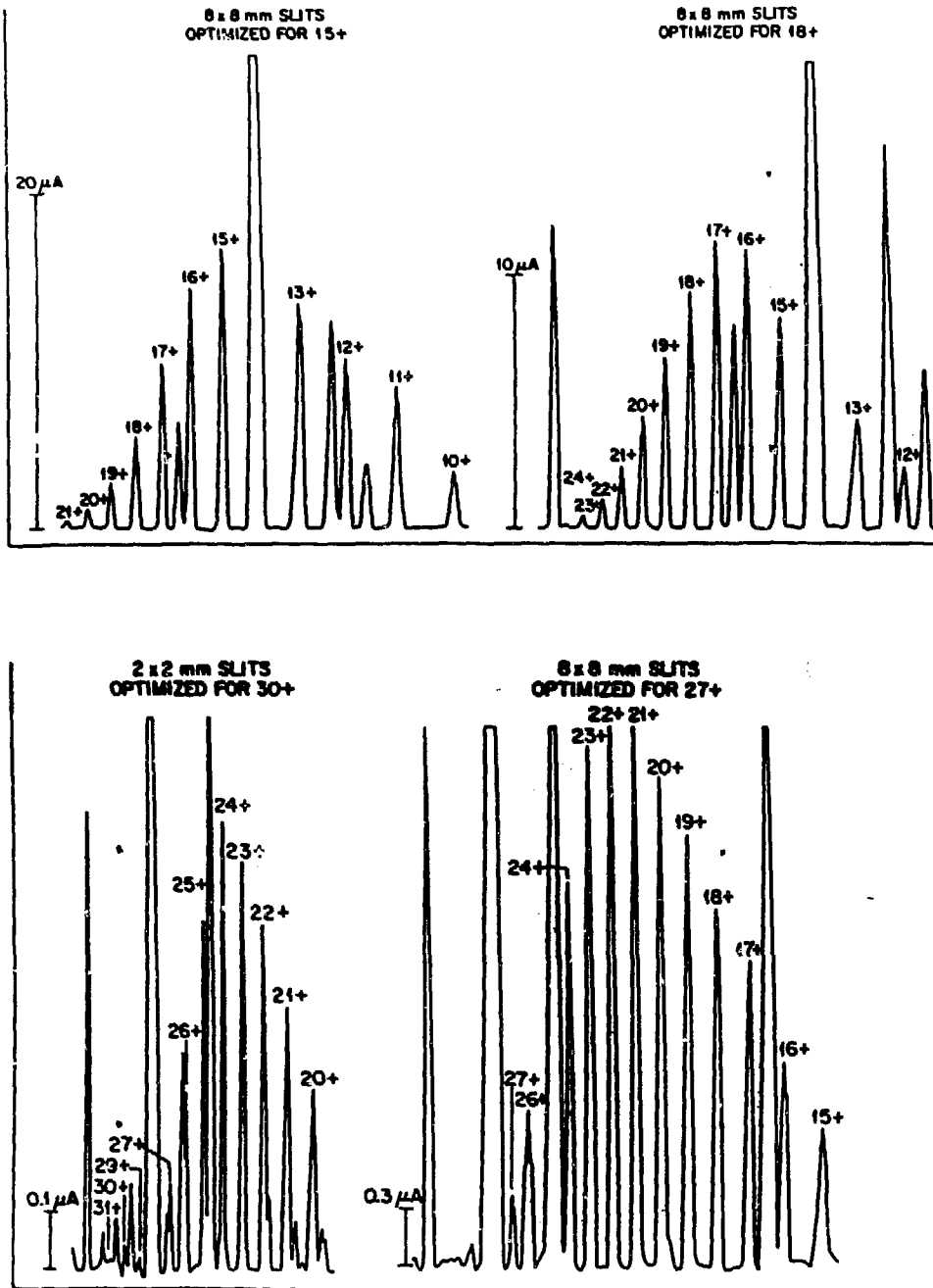


Fig. 4. Charge state distributions of Au ions extracted from the ORNL ECR source, for four different source conditions.

thereby expanding the ECR plasma toward the Ta liner until sufficient interaction took place for wall material "recycling." The Au sample used consisted of 0.5 mm wire wound around a matrix of two 0.8 mm W rods, the free ends of which were then clamped to the foil positioning mechanism. In the case of the Au ions, a large variation in sample position was required in order to optimize different charge states, low charge states requiring the sample to be inserted significantly farther into the plasma to generate sufficient Au vapor density than the highest charge states. Figure 4 shows sample charge state distributions obtained for gold ions under different source conditions.

The day to day reliability of the ORNL ECR source has been extremely good. Cleaning of the source is required only after many weeks of metal ion production. Source opening is required to change solid feed materials, but this is accomplished conveniently and quickly. Typical cycle times required by two people to change samples are about half an hour.

## Multicharged Ion Collision Physics

### Ion-Atom Interactions

One of the unique capabilities of ECR sources is the ability to produce copious quantities of fully stripped ions with atomic number up to about 10. This capability makes possible experiments studying the atomic collisional interactions of few-electron systems. Such systems are of significant fundamental interest, since they are most amenable to calculation.

One example of this class of experiments is the study of single electron capture by bare nuclei in slow collisions with atomic hydrogen. These collision systems, which include only one electron, and which are one of the simplest in atomic collision physics, have been calculated using a number of different theoretical methods. Experimental validation of these calculations was only recently made possible by the development of advanced multicharged ion sources such as the ECRIS.

Figure 5 shows the experimental setup used at Oak Ridge to measure total electron capture cross sections for the above collision systems. The atomic hydrogen target is produced by thermal dissociation of molecular hydrogen in a W tube heated to roughly 2500 K. Figure 6 shows the charge dependence of the experimentally determined total cross sections, both for

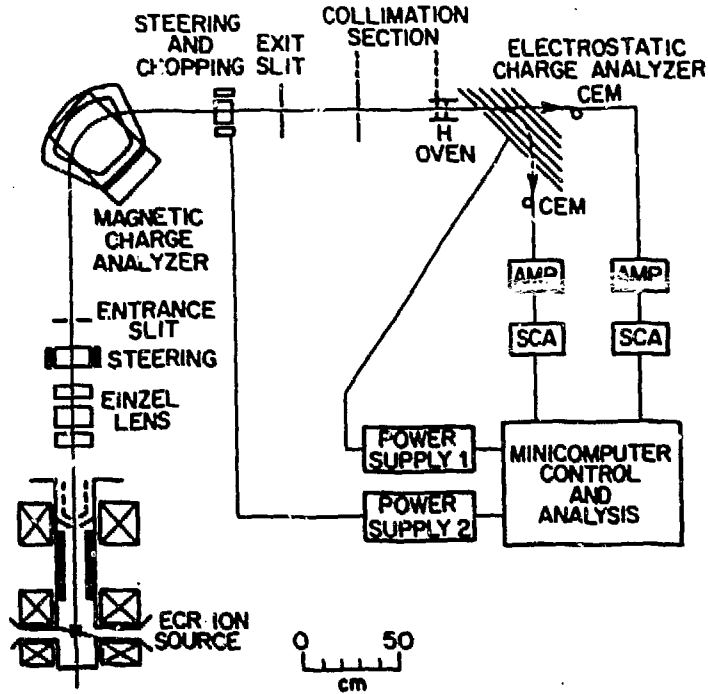
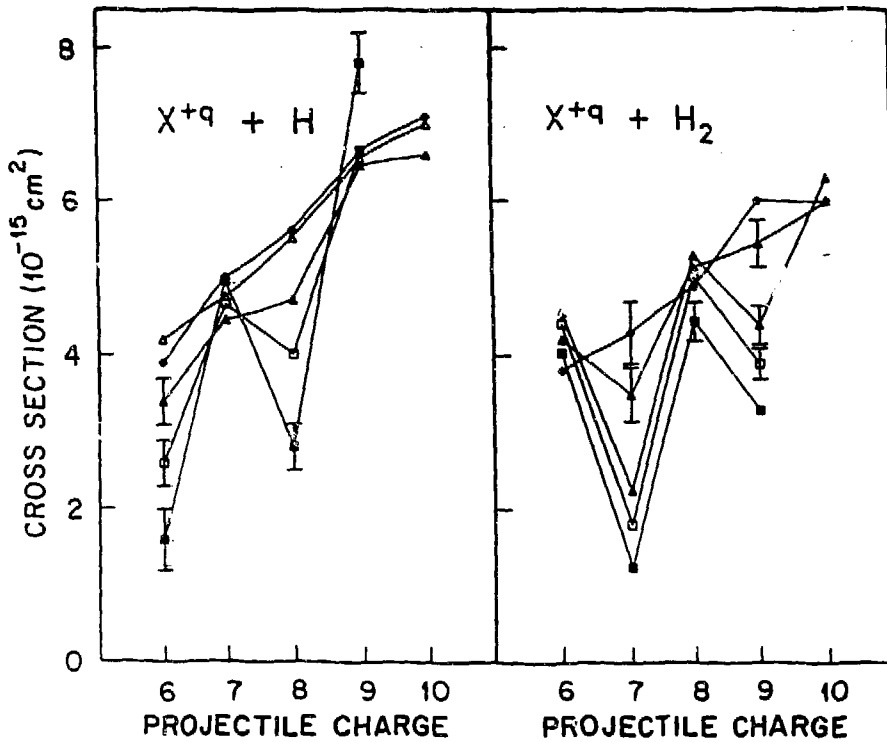


Fig. 5. Schematic layout of apparatus for measurement of total capture cross sections with H target.



Charge dependence of experimental total electron capture cross sections for fully stripped projectiles ( $6 < Z < 10$ ) incident on H and  $H_2$ .  $\blacksquare$  - 0.3 keV/amu;  $\square$  - 0.6 keV/amu;  $\blacktriangle$  - 1.0 keV/amu;  $\triangle$  - 3.0 keV/amu;  $\blacklozenge$  - 8.0 keV/amu. A few representative error bars are indicated.

Fig. 6.

atomic and molecular hydrogen targets, at a number of different collision energies. The pronounced oscillations in the q-scaling at the lower energies arise as a result of the strong final state selectivity of the capture process at low energies, and have been analyzed in Ref. 2. Less comprehensive measurements of total capture cross sections for fully stripped ions incident on atomic hydrogen were also carried out in Grenoble<sup>9</sup> and Groningen.<sup>10</sup> In addition, line emission cross sections were measured at Groningen<sup>10</sup> for some of the above collision systems, by which the final n state populated in these single electron capture collisions could be deduced, thereby providing a more severe test of the various theoretical treatments of electron capture in these one electron systems.

There is also significant interest in the mechanisms of electron transfer that become important at energies lower than those that can be investigated in beam-gas target experiments. While at the energies investigated in the above measurements the trajectories of the two collision partners can be theoretically treated by impact parameter or other semiclassical approximations, at sufficiently low collision energies, a quantum-mechanical treatment is required not only for the dynamical interaction between the initial channel and the manifold of final states, but also for the trajectories of the collision partners during the interaction. Theoretical treatments of electron transfer in this energy regime are quite difficult and require experimental benchmark data for validation. There is also applied interest in very low energy charge transfer, due to its dominant role in determining the characteristics of the part of the plasma in closest proximity to the wall of fusion reactors, where atomic hydrogen wall recycling and radiative losses by charge exchange excitation of partially stripped impurity ions are important issues.

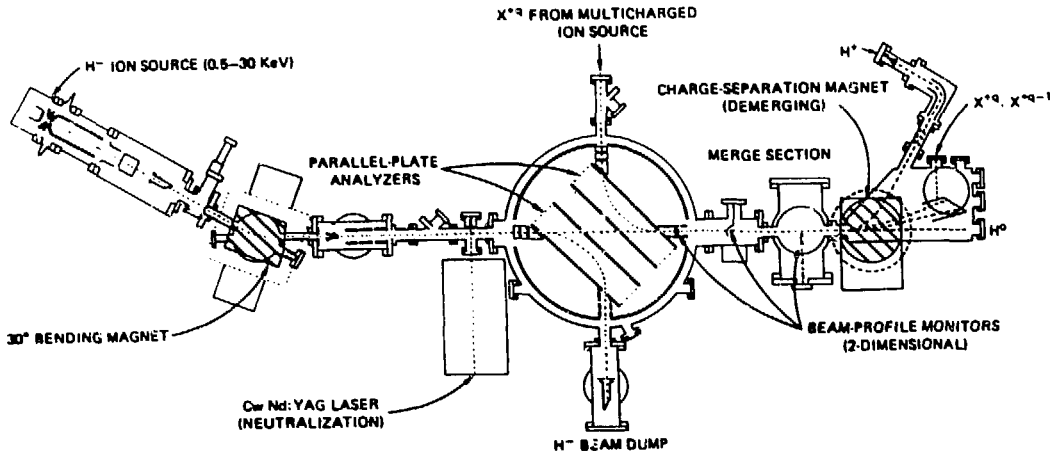
The very low energy regime is demanding also experimentally. Especially when dealing with collisions involving atomic hydrogen, merged ion-atom beam experiments are required, in which two relatively fast beams are merged and allowed to interact at arbitrarily low relative velocity determined by the difference in laboratory velocities of the two beams. Due to the nature of the kinematical transformation from the center of mass frame in which the collisions occur to the laboratory frame in which the collision products are detected, the merged beams technique affords the capability of efficient collection of collision products that have suffered

significant angular scattering during the collision, an important consideration when studying low energy collisions. Due to the tenuous nature of the "target," the merged beams technique is characterized by inherently low signal rates, thus requiring ion beams of good stability and high intensity. The technique has become experimentally feasible for studying low energy multicharged ion collisions only since the advent of the ECR source, which is capable of satisfying these requirements.

Figure 7 shows a schematic diagram of a merged beams apparatus<sup>8</sup> developed at Oak Ridge for the study of electron capture by partially stripped projectiles from atomic hydrogen at relative collision energies as low as fractions of an eV/amu. The fast atomic hydrogen beam is formed by photo-detachment of H<sup>-</sup> using a high power Nd:YAG laser. The merged path over which the two beams interact is almost 1 m in length. In order to obtain reliable cross sections using this technique, the overlap of the two beams must be accurately known along the entire merged path. In the present experiment, this is accomplished by the use of a combination of commercial rotating wire beam scanners and stepping-motor-controlled knife edges, by means of which two orthogonal profiles of the two beams are measured at four different locations along the merge path. Figure 8 shows some sample beam profiles obtained using the two types of beam scanners.

Sample data obtained with this apparatus is shown in Figure 9 for O<sup>8+</sup> + H collisions.<sup>11</sup> As can be seen from the measurements, which cover the range 1 to 1000 eV/amu, the merged beam technique has a very large dynamic range. At the very lowest energies investigated, the cross section is seen to rise steeply with decreasing energy. This feature may be evidence for enhancement of electron transfer by trajectory effects: at sufficiently low energies the polarization interaction between the multicharged ion and the neutral hydrogen atom is sufficiently strong to result in a temporary capture of the H atom. During this time interval, the two collision partners orbit about each other, significantly increasing the time available for electron transfer.

In order to obtain information on the specific final states populated in multicharged ion collisions, a variety of spectroscopic methods have been developed, based on analysis of projectile kinetic energy change, or of photon or electron emission resulting from the collision. Optical and electron spectroscopy offer potentially high resolution, but suffer from



**ION-ATOM MERGED-BEAMS EXPERIMENT**

Fig. 7. The ORNL merged beams experiment.

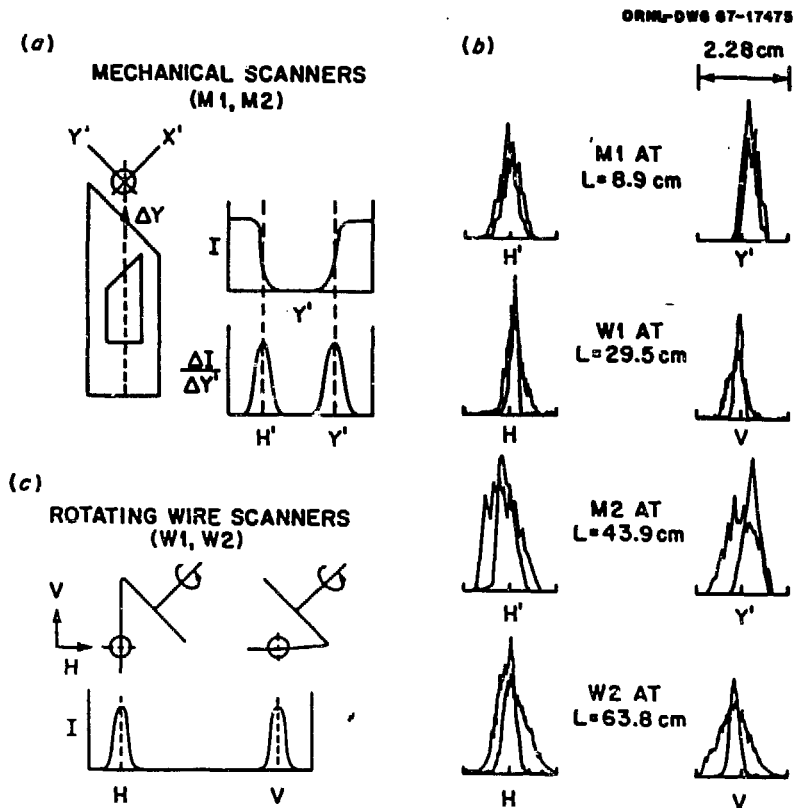


Fig. 8. Sample beam overlap scans along merge path.

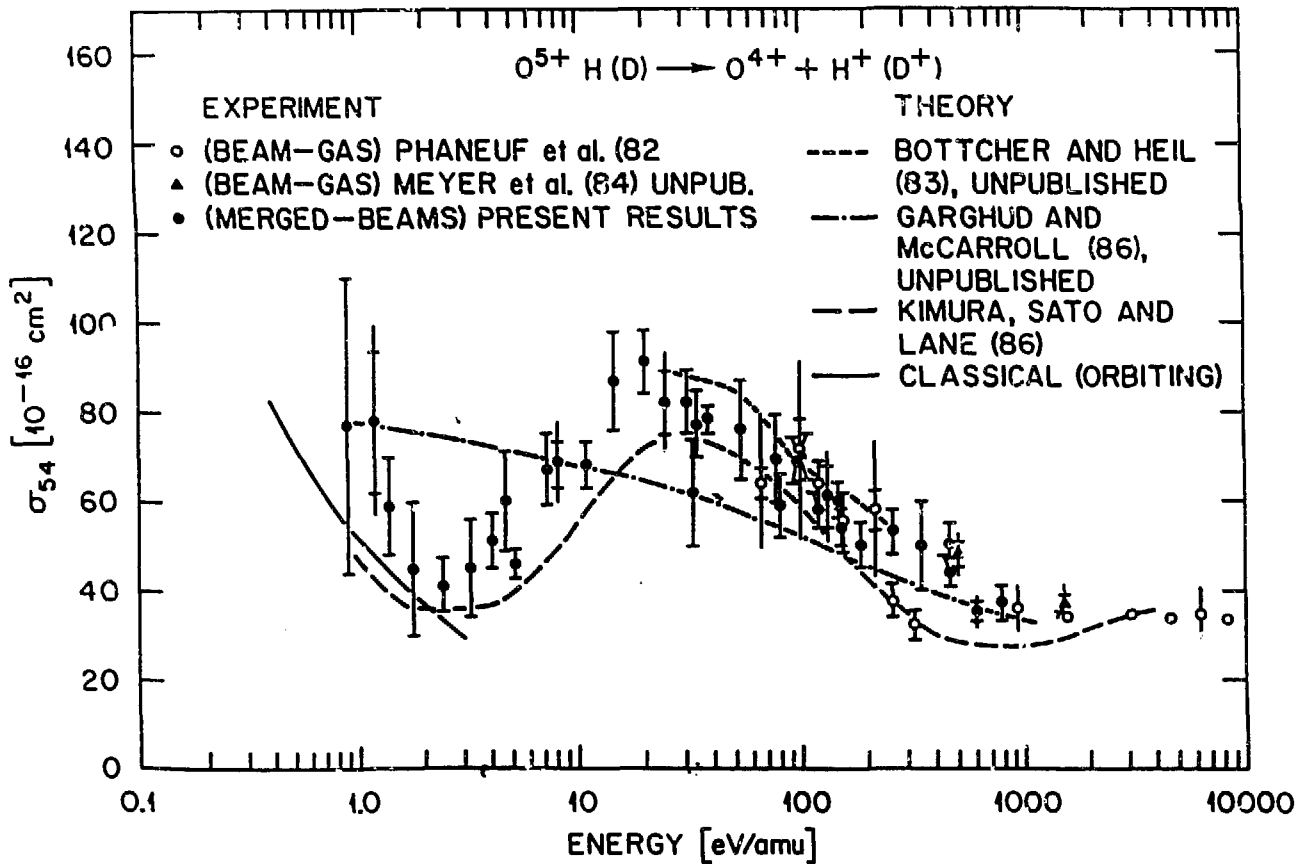


Fig. 9. Total electron capture cross section for  $O^{5+} + H$  collisions measured using merged beams technique.

low collection efficiency. As a result, high beam intensities are prerequisites.

In addition to the VUV spectroscopic measurements of electron capture collisions at Groningen already referred to above, measurements in the XUV and X-ray region are being carried out at Grenoble, where they are used not only as probes of collisions, but also as means of identification<sup>12</sup> of very highly stripped ion beams that are either poorly resolved from neighboring beams or have some contamination due to  $m/q$  degeneracies.

The technique of Auger electron spectroscopy has also seen increasing use in the study of low energy multicharged ion collisions. Starting with the measurements of Bordenave-Montesquieu at Grenoble,<sup>13</sup> this technique is being used at a number of ECR facilities to study the formation of autoionizing states in multicharged ions. In particular, electron spectroscopy has proven to be a very powerful tool in the study of double-electron capture collisions. The analysis of the classes of doubly excited (i.e., autoionizing) final states formed in such collisions by the use of electron spectroscopy gives information on the various mechanisms active in double capture collisions which at present are still not very well understood.

Figure 10 shows the schematic of an Oak Ridge experiment used to study Auger electrons emitted as a result of multicharged ion collisions with a variety of target gases. A typical electron spectrum produced in  $O^{8+} + He$  collisions is shown in Fig. 11. An analysis<sup>14</sup> of this collision system has shown that the so-called non-equivalent configurations that decay by emission of L-Coster-Kronig electrons can only be populated by a correlated electron process, the first time that a specific mechanism for double electron capture could be unambiguously identified.

### Electron-Ion Collisions

Another area of multicharged ion collision physics in which ECR sources have already had significant impact is that of electron-ion interactions. In particular, great progress has been made in the study of electron impact ionization of multicharged ions. Electron-ion collisions play an important role in determining the ionization balance of impurity ions in fusion plasmas, and affect sensitively the power loss by optical radiation from electronically excited impurity species. The strong fusion interest in electron-ion collisions dates back to confinement experiments



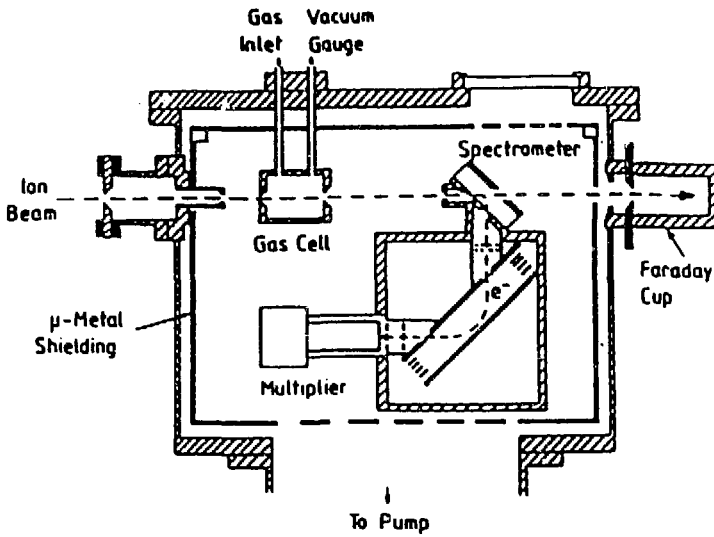


Fig. 10. Auger electron spectrometer setup used at ORNL ECR source facility.

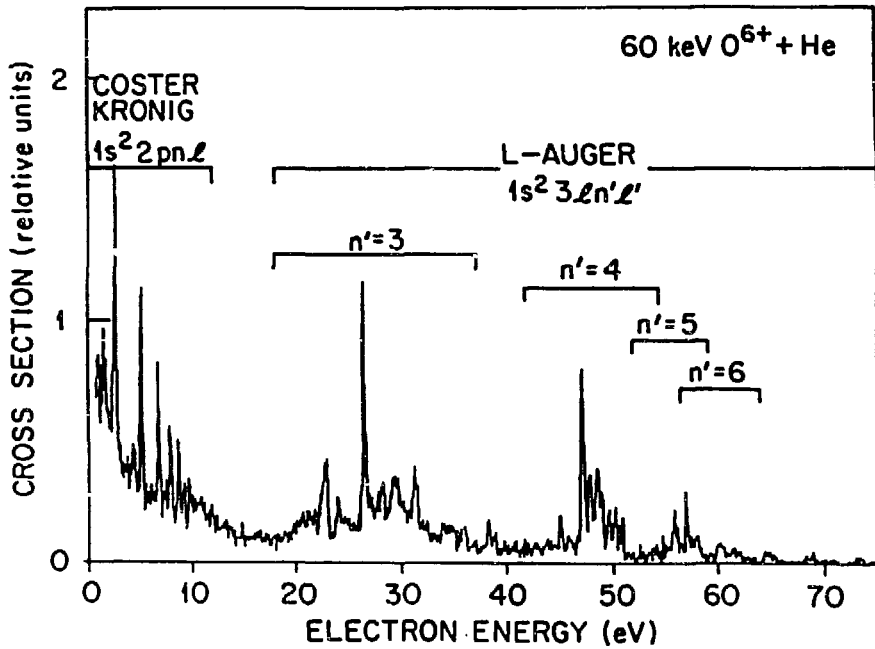


Fig. 11. Measured high resolution electron spectrum for 60 keV  $O^{6+} + He$  collisions.

performed on the ORMAK tokamak at Oak Ridge in the early 1970's. The ORMAK device, featuring plasma limiters made from tungsten, was unable to attain the ion temperatures theoretically predicted on the basis of the known power input, indicating unexpectedly high power losses from the plasma. The culprit was finally discovered to be line radiation from excited states of very high ionization stages of W, which accounted for more than 50% of the total applied heating power! The trend in the design of fusion devices since then has been to lower Z materials; nevertheless, interactions of impurity ions and their control in fusion plasmas are still important issues today.

Driven by the strong applied interest, a long term program to study electron impact ionization has been underway at Oak Ridge for the past 10 years. Figure 12 shows the most recent configuration of the experimental apparatus used in these investigations. Recent focus of the program has been a comprehensive study of indirect ionization mechanisms in electron-multicharged ion collisions. Of specific interest has been the mechanism of inner shell excitation followed by autoionization of the resulting doubly excited state. For certain ions, this mechanism was found to enhance the total electron impact ionization cross section by more than an order of magnitude! By systematic measurements along isonuclear and isoelectronic sequences, and guided by close interaction with atomic structure theorists, a better understanding has emerged of the set of conditions under which indirect ionization mechanisms play significant roles. Figure 13 shows electron impact ionization cross sections measured<sup>15</sup> along the Ni isonuclear sequence. For Ni<sup>3+</sup> ions, the cross section is well described by direct ionization of a 3d electron. This direct mechanism underestimates the total observed ionization by varying amounts for the higher charge states. For Ni<sup>12+</sup> and Ni<sup>14+</sup> the characteristic onset for excitation-autoionization is observed, as an inner shell 2p electron is excited into the 3p or 3d level, forming a doubly excited state which rapidly autoionizes, leading to the net loss of an electron, i.e., an ionization event. In Fig. 14 the magnitude of the excitation-autoionization contribution is explored along the Ti<sup>11+</sup>, Cr<sup>13+</sup>, Fe<sup>15+</sup> Na-like isoelectronic sequence (i.e., same electronic configuration, but different charge). Note the order of magnitude enhancement of the ionization cross section for Ti<sup>11+</sup> due to the indirect mechanism.

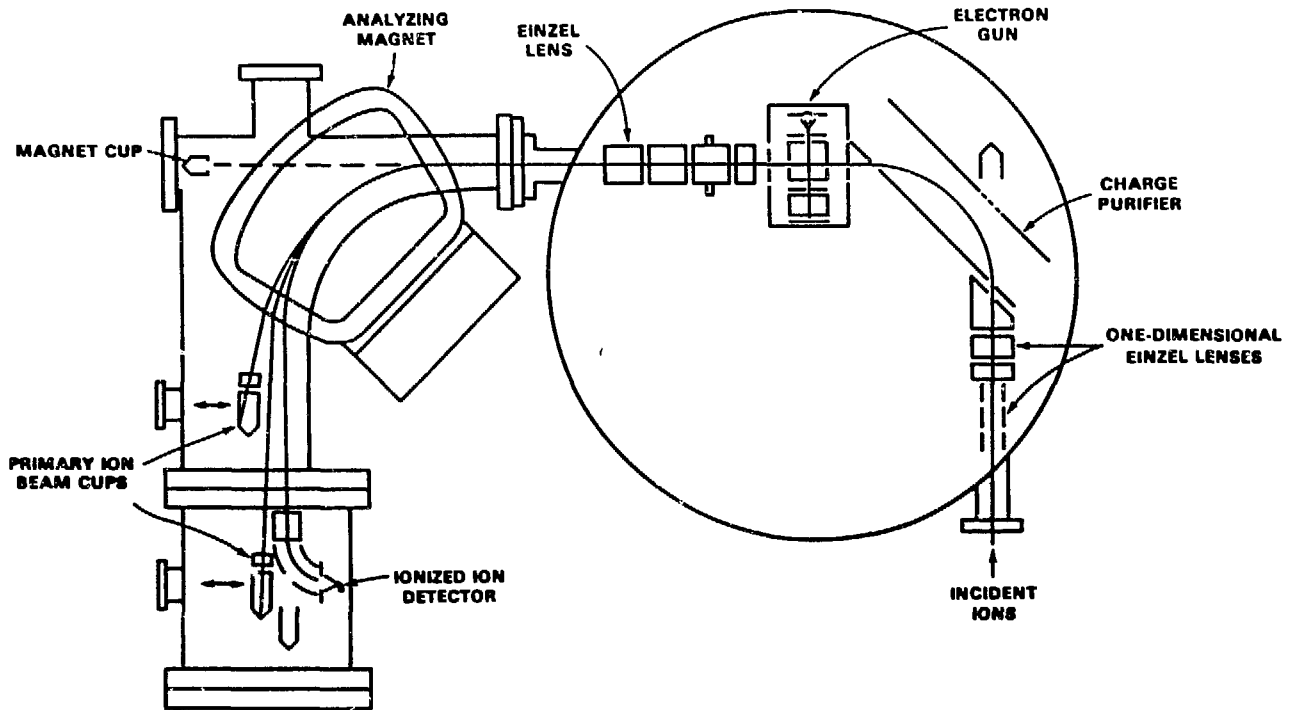


Fig. 12. The ORNL crossed electron-ion beams experimental setup.

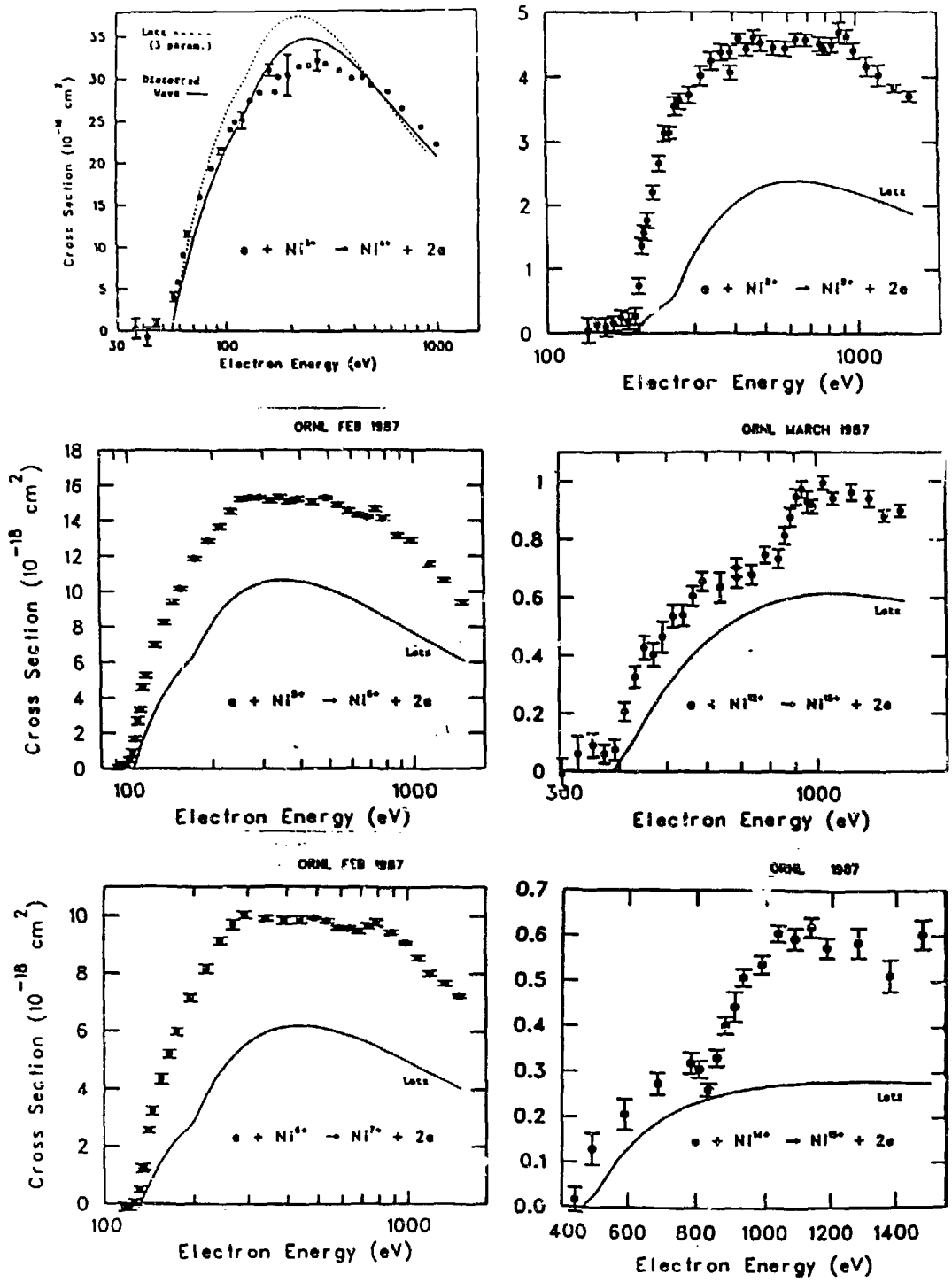
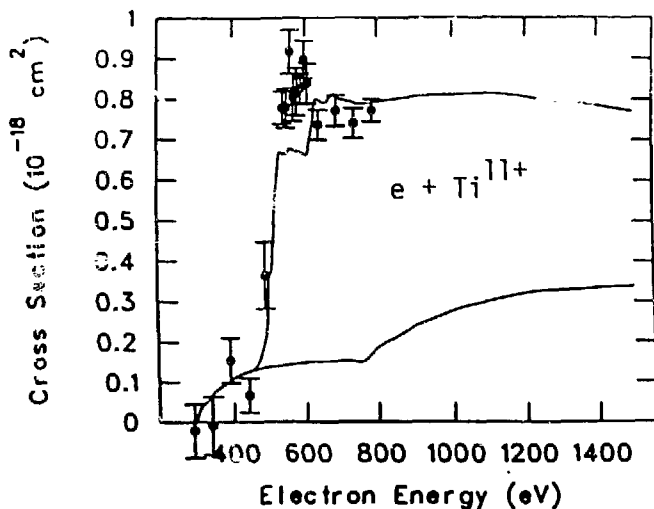


Fig. 13. Measured electron impact ionization cross sections for the Ni isonuclear sequence.

ORNL AUG 1987



ORNL NOV 1987

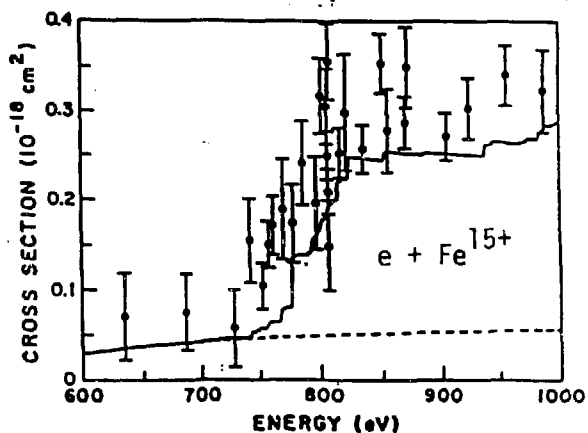
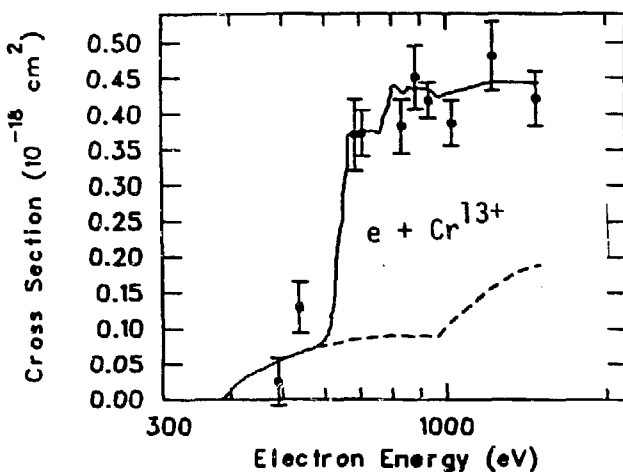


Fig. 14. Measured electron impact ionization cross sections along the Na-like isoelectronic sequence  $\text{Ti}^{11+}$ ,  $\text{Cr}^{13+}$ ,  $\text{Fe}^{15+}$ . The Ti and Cr data are preliminary, unpublished data by D. C. Gregory et al.

As can be seen from Table I, electron-ion collisions are being investigated using ECR sources also at Louvain-la-Neuve and Giessen. To date, only the Oak Ridge program has carried out measurements on metal ions, or investigated ionic charge states greater than 9+.

### Surface Collisions

The study of multicharged ion-surface interactions is of considerable current interest, in large part due to the significant neutralization potential energy that the multicharged projectiles carry into the collision. The detailed mechanisms by which this potential energy is dissipated and in the process affects electron ejection, ion neutralization, sputtering, or reflection during the surface interaction are still incompletely understood, making this a very fertile area of experimental as well as theoretical investigation. At Groningen,<sup>16</sup> ion reflection and electron emission during multicharged ion-surface collisions have been studied for a number of years. Total secondary electron yields as well as electron energy distributions have been measured at Grenoble,<sup>17</sup> also as part of an ongoing program.

At Oak Ridge, measurements<sup>18</sup> have been performed over the past two years in collaboration with University of Osnabrück researchers whose aim was the study of the neutralization of ions carrying into the surface collision deep lying K- or L-shell vacancies. A surprising result of this investigation was that these initial vacancies are filled not only by normal Auger decay subsequent to the filling of the outer shells of the projectile by resonant capture from the valence band of the solid, but also by direct vacancy transfer reactions with inner shells of atoms of the bulk material or of surface adsorbates. These inner shell reactions are quite selective, and suggest the interesting possibility of using multicharged ions as surface probes.

Figure 15 shows the experimental setup used to study multicharged ion-surface collisions at Oak Ridge. The projectiles collide with a clean Au surface at grazing incidence. The ejected electrons are energy analyzed using a cylindrical mirror analyzer. A typical electron energy distribution for  $O^{7+}$  incident ions is shown in Fig. 16. Note that in addition to the expected oxygen KLL Auger electrons around 500 eV, there are peaks in the electron distribution at lower energies associated with the decay of inner shell vacancies in Au. The Au vacancies were created by vacancy transfer via molecular orbital pseudocrossings as illustrated in Fig. 17.

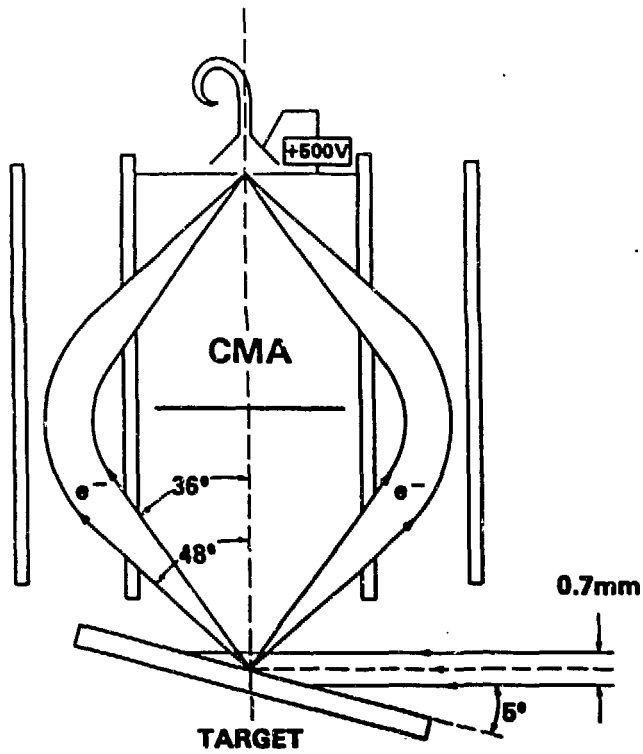


Fig. 15. Apparatus used for multicharged ion-surface measurements at Oak Ridge.

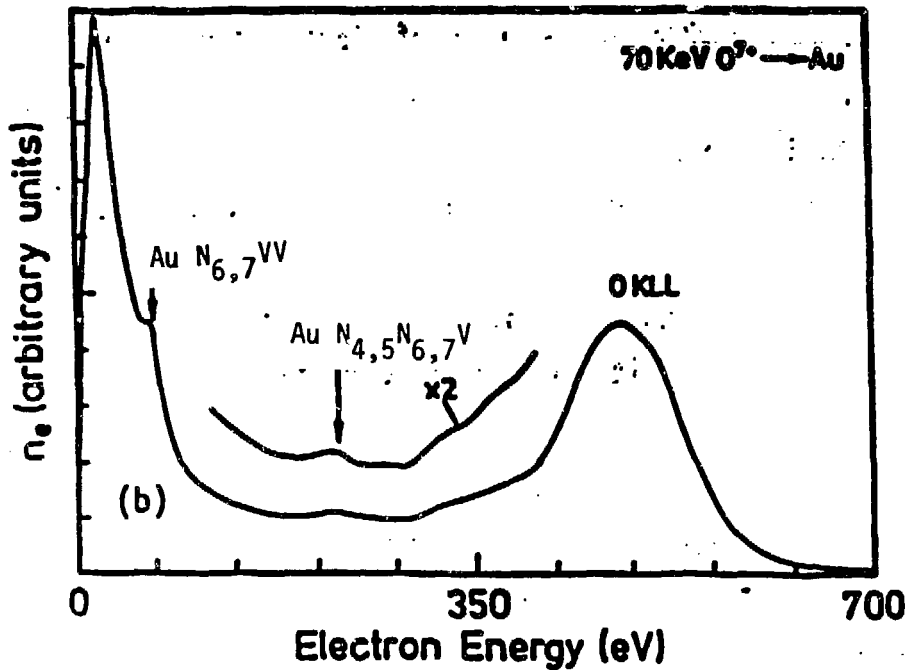


Fig. 16. Measured electron energy distribution for 70 keV  $O^{7+}$  incident on a clean Au surface at  $5^\circ$ .

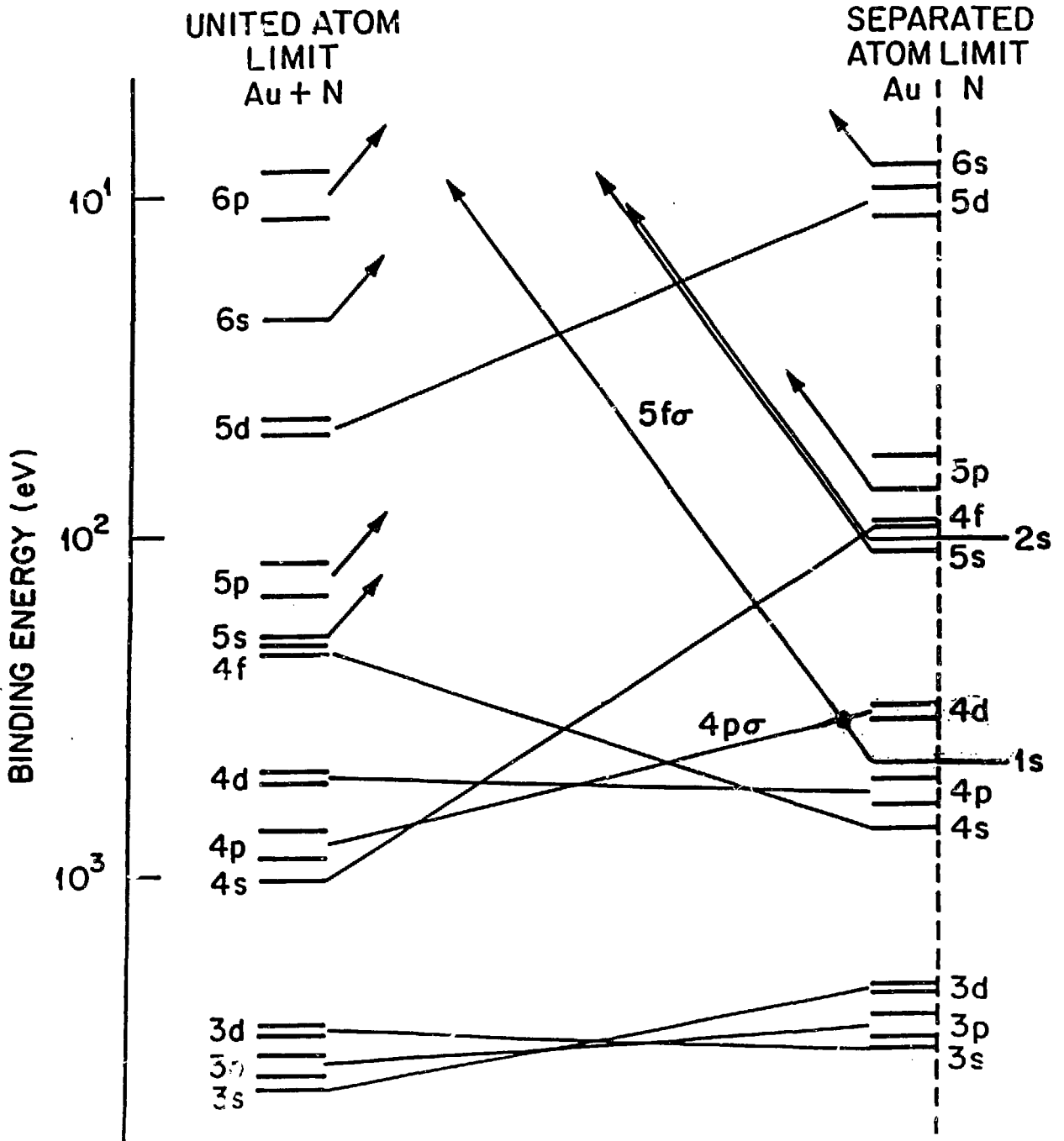


Fig. 17. N-Au correlation diagram, showing the pathway for vacancy transfer from the 1s shell of N to the 4d shell of Au.



ORNL-DWG 87-13357

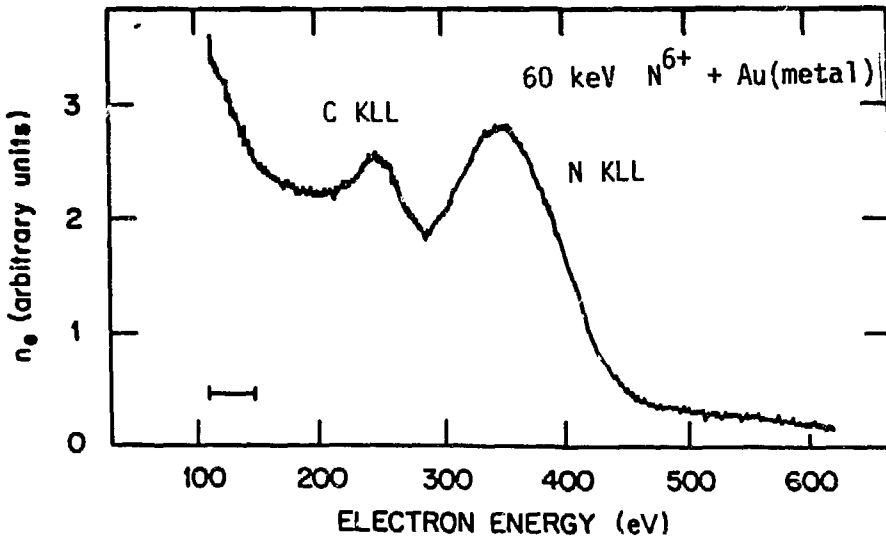
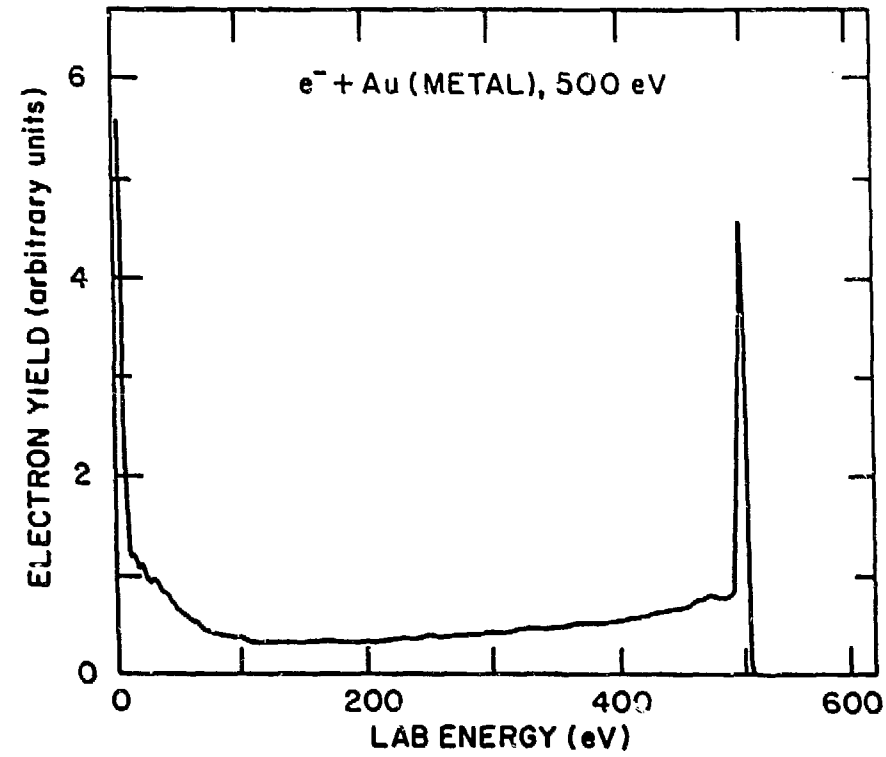


Fig. 18. Comparison of electron induced and multicharged ion induced Auger electron spectrum for a gold surface covered with a 20% monolayer of carbon.

In conventional electron-induced Auger electron spectroscopy the yield of characteristic target Auger electrons is significantly lower, requiring the use of special signal recovery techniques such as phase sensitive detection. Figure 18 shows a comparison between electron induced and multi-charged ion induced electron spectra for a "dirty" Au surface having 20% monolayer coverage of carbon. The single narrow peak at 500 eV in the electron induced spectrum is the elastic backscattering peak, whose height represents the incident electron intensity. There are no additional discrete features easily discernible in this spectrum. The  $N^{6+}$  induced electron spectrum, on the other hand, shows in addition to the expected nitrogen KLL Auger peak at about 350 eV, whose yield per incident ion is close to unity, a very pronounced carbon KLL peak. By comparison with the N KLL peak height, a carbon KLL yield of about 30% is inferred, making the  $N^{6+}$  ion an extremely sensitive probe of carbon contamination.

### Summary

After a brief overview of the ORNL ECR source facility, some highlights were given of the atomic physics application of ECR ion source beams, based on multicharged ion collision experiments carried out at Oak Ridge in recent years. The discussion could of necessity not be complete and was intended to be only illustrative in nature. As was pointed out, there are many ECR source facilities at which atomic physics experiments are being carried out, studying the collisional properties of multicharged ions as well as various aspects of their atomic structure with a wide variety of experimental techniques. Multicharged ion research has been one of the most rapidly growing areas of atomic physics in recent years. As ECR source design continues to evolve and provide ever improving performance, ECR source based atomic physics will continue to be a research area of rapid growth and unrivaled vitality.

### References

\*Operated by Martin Marietta Energy Systems, Inc. for the U. S. Department of Energy under contract No. DE-AC05-84OR21400.

1. F. W. Meyer, Nucl. Instrum. Methods B9, 532 (1985).
2. F. W. Meyer, A. M. Howalu, C. C. Havener, and R. A. Phaneuf, Phys. Rev. Lett. 54, 2663 (1985).

3. A. M. Howald, D. C. Gregory, F. W. Meyer, R. A. Phaneuf, A. Mueller, N. Djuric, and G. H. Dunn, *Phys. Rev. A* **33**, 3779 (1986).
4. C. C. Havener, P. A. Schulz, and R. A. Phaneuf, *Bull. Am. Soc.* **31**, 974 (1986).
5. D. C. Gregory, F. W. Meyer, A. Mueller, and P. Defrance, *Phys. Rev. A* **34**, 3657 (1986); D. C. Gregory, L. J. Wang, F. W. Meyer, and K. Rinn, *Phys. Rev. A* **35**, 3256 (1987).
6. F. W. Meyer, *Contributed Papers of the 7th Workshop on ECR Ion Sources*, H. Beuscher, editor, 22-23 May 1986, Jülich, Fed. Rep. Germany, Jülich Report ISSN 0344-5798, p. 10.
7. F. W. Meyer, *Proceedings of 5th ECR Ion Sources Workshop*, Louvain-la-Neuve, Belgium, April 21-22, 1983.
8. M. Delaunay, S. Dousson, R. Geller, and B. Jacquot, *Nucl. Instrum. Methods* **213**, 165 (1983).
9. M. Bendahman, S. Bliman, S. Dousson, D. Hitz, R. Gayet, J. Hanssen, C. Harel, and A. Salin, *J. Phys. (Paris)* **46**, 561 (1985).
10. D. Dijkamp, D. Ciric, and F. J. de Heer, *Phys. Rev. Lett.* **54**, 1004 (1985).
11. C. C. Havener, M. S. Huq, and R. A. Phaneuf, *Abstracts of Contributed Papers, XV ICPEAC, Brighton, England*, p. 529, and *Physical Review A*, to be published.
12. F. Bourg, P. Briand, J. Debernardi, R. Geller, B. Jacquot, P. Ludwig, M. Pntonier, and P. Sortais, *Contributed Papers of the 7th Workshop on ECR Ion Sources*, H. Beuscher, editor, 22-23 May, 1986, Jülich, Fed. Rep. Germ. Jülich Rep. ISSN 0344-5798, p. 187.
13. A. Bordenave-Montesquieu, P. Benoit-Cattin, A. Gleizes, A. I. Marrachi, S. Dousson, and D. Hitz, *J. Phys.* **B17**, L127 (1984); **B17**, L223 (1984); **B18**, L195 (1985).
14. For example, M. Mack and A. Niehaus, *Nucl. Instrum. Methods* **B23**, 116 (1987).
15. F. W. Meyer, C. C. Havener, R. A. Phaneuf, J. K. Swenson, S. M. Shafroth, *Nucl. Instrum. Methods* **B24/25**, 106 (1987).
16. P. C. Kester, R. Schulze, and E. Salzborn, *Abstracts of Contributed Papers, XV ICPEAC, Brighton, England*, p. 434.
17. N. Stolterfoht, C. C. Havener, R. A. Phaneuf, J. K. Swenson, S. M. Shafroth, and F. W. Meyer, *Phys. Rev. Lett.* **57**, 74 (1986).
18. L. J. Wang, K. Rinn, and D. C. Gregory, *Physical Review A*, to be published.
19. S. T. de Zwart, T. Fried, U. Jellen, A. L. Boers, and A. G. Drentje, *J. Phys. B* **18**, L623 (1985); S. T. de Zwart, Ph.D. Thesis, University of Groningen, 1985.
20. M. Delaunay, M. Fehringer, R. Geller, D. Hitz, P. Varga, and H. Winter, *Phys. Rev. B* **35**, 4232 (1987); also, M. Delaunay, R. Geller, J. Debernardi, and P. Sortais, *proceedings of this conference*.
21. For example, F. W. Meyer, C. C. Havener, K. J. Snowdon, S. H. Overbury, D. Zehner, and W. Heiland, *Phys. Rev. A* **35**, 3176 (1987).